HHS Public Access

Author manuscript

Cell Rep. Author manuscript; available in PMC 2016 January 25.

Published in final edited form as:

Cell Rep. 2016 January 12; 14(2): 180–188. doi:10.1016/j.celrep.2015.12.035.

The Mid2 X-linked Intellectual Disability Ubiquitin Ligase Associates with Astrin and Regulates Astrin Levels to Promote Cell Division

Ankur A. Gholkar[1], **Silvia Senese**[1], **Yu-Chen Lo**[1,2], **Edmundo Vides**[1], **Ely Contreras**[1], **Emmanuelle Hodara**[1], **Joseph Capri**[3], **Julian P. Whitelegge**[3,4,5], and **Jorge Z. Torres**[1,4,5,*]

[1]Department of Chemistry and Biochemistry, University of California, Los Angeles, CA 90095, USA

[2]Program in Bioengineering, University of California, Los Angeles, CA 90095, USA

[3]Pasarow Mass Spectrometry Laboratory, The Jane and Terry Semel Institute for Neuroscience and Human Behavior, David Geffen School of Medicine, University of California, Los Angeles, CA 90095, USA

[4]Molecular Biology Institute, University of California, Los Angeles, CA 90095, USA

[5]Jonsson Comprehensive Cancer Center, University of California, Los Angeles, CA 90095, USA

SUMMARY

Mid1 and Mid2 are ubiquitin ligases that regulate microtubule dynamics and whose mutation is associated with X-linked developmental disorders. We show that Astrin, a microtubule-organizing protein, co-purifies with Mid1 and Mid2, has an overlapping localization with Mid1 and Mid2 at intercellular bridge microtubules, is ubiquitinated by Mid2 on lysine 409 and is degraded during cytokinesis. Mid2 depletion led to Astrin stabilization during cytokinesis, cytokinetic defects, multinucleated cells, and cell death. Similarly, expression of a K409A mutant Astrin in Astrin-depleted cells led to the accumulation of K409A on intercellular bridge microtubules and an increase in cytokinetic defects, multinucleated cells, and cell death. These results indicate that Mid2 regulates cell division through the ubiquitination of Astrin on K409, which is critical for its degradation and proper cytokinesis. These results may help explain how mutation of *MID2* leads to misregulation of microtubule organization and the downstream disease pathology associated with X-linked intellectual disabilities.

*Corresponding author: Jorge Z. Torres, 607 Charles E. Young Drive East, Los Angeles, CA 90095, Phone: 310-206-2092, Fax: 310-206-5213, torres@chem.ucla.edu.

AUTHOR CONTRIBUTIONS

AAG, SS, YL, EV, EC, EH, JC, JPW and JZT performed experiments and discussed results. AAG, SS and JZT wrote the paper with input from YL, EV, EC, EH, JC and JPW.

SUPPLEMENTAL INFORMATION

Supplemental Information includes Supplemental Experimental Procedures, 4 figures, one table and 6 movies.

Keywords

Mid2; Astrin; X-linked intellectual disability; Cell division; Cytokinesis

INTRODUCTION

The TRIM/RBCC (tripartite motif composed of a RING finger, zinc binding motif/s called B-box/s, and a coiled coil region) superfamily of E3 ubiquitin ligases have variable roles in cellular homeostasis including signaling, regulation of cytoskeletal structures and cell cycle progression (Meroni and Diez-Roux, 2005). The Mid1 (Midline 1, aka Trim18) and Mid2 (Midline 2, aka Trim1) ubiquitin ligases belong to the C-I TRIM subfamily and share a similar domain architecture, with an N-terminal tripartite motif and FN3 (fibronectin type III) and B30.2-like/RFP (Ret finger protein) domains at their C-terminus (Meroni and Diez-Roux, 2005) (Figure 1A). Mid1 and Mid2 also contain a COS (C-terminal subgroup one signature) box between the coiled coil and FN3 motif that mediates the binding of these proteins to microtubules (Short and Cox, 2006) (Figure 1A).

Mid1 and Mid2 have critical roles during development and mutation of *MID1* has been linked to Opitz syndrome (MIM#300000), an X-linked disease characterized by congenital anomalies that is manifested by the abnormal closure of midline structures (Cainarca et al., 1999), whereas mutation of *MID2* has been linked to X-linked intellectual disabilities (MIM #300204) (Geetha et al., 2014). Mid1 and Mid2 homo and heterodimerize (Cainarca et al., 1999; Short et al., 2002) and have been implicated in anchoring proteins to microtubules, in bundling and stabilizing of microtubules, and in organizing microtubules during neural tube closure (Berti et al., 2004; Short et al., 2002; Suzuki et al., 2010). Therefore, Mid1 and Mid2 have roles in microtubule stability and organization, however whether their ubiquitin ligase activities are required for regulating these processes remains to be determined. Although, Mid1 ubiquitination substrates include alpha4, the catalytic subunit of protein phosphatase 2A, and Fu, whether ubiquitination of these proteins leads to changes in microtubule organization has not been explored (Du et al., 2013; Schweiger et al., 2014; Trockenbacher et al., 2001). Additionally, to our knowledge, there are no known substrates of Mid2 that can explain its role in regulating microtubule organization.

To better understand the molecular basis of X-linked developmental diseases associated with mutation of *MID1* and *MID2*, we analyzed the Mid1 and Mid2 interactomes and identified SPAG5 (sperm associated antigen 5, aka hMAP126 and Astrin). Astrin is a microtubule bundling/organizing protein critical for regulating microtubules during cell division (Gruber et al., 2002; Mack and Compton, 2001; Thein et al., 2007). Mid1 and Mid2 showed an overlapping localization with Astrin to intercellular bridge microtubules (ICBMTs). Depletion of Mid1 or Mid2 arrested cells during cytokinesis and generated binucleated cells. Importantly, Mid2 ubiquitinated Astrin on lysine 409 during mitotic exit and was required for Astrin degradation. Experiments where endogenous Astrin was depleted and wildtype or a K409A (Mid2 ubiquitination resistant mutant) Astrin were reintroduced showed that Astrin-K409A accumulated at ICBMTs, arrested cells during cytokinesis, and led to an increase in binucleated cells and cell death. These data indicate that Mid2 ubiquitinates and

targets a pool of Astrin for degradation during cytokinesis, which is important for proper cytokinesis.

RESULTS

Mid1 and Mid2 Associate with Astrin

To understand the molecular basis of X-linked developmental disorders associated with mutation of *MID1* and *MID2*, we began by defining the Mid1 and Mid2 interacting proteins. HEK293 doxycycline-inducible localization and affinity purification (LAP= EGFP-TEV-S-Peptide)-tagged Mid1 and Mid2 stable cell lines were used to express and tandem affinity purify LAP-Mid1/Mid2 (Torres et al., 2009). Eluates were resolved by SDS-PAGE and ten gel slices were excised and analyzed individually by mass spectrometry (Figure 1B). Cytoscape data analysis showed that Mid1 and Mid2 associated with each other, as reported previously (Short et al., 2002), and with proteasome subunits, tubulin and Astrin, while Mid2 also associated with the centrosomal proteins ASPM and Cep128 (Figures 1C and 1D; Table S1). Due to Astrin's role in crosslinking/bundling microtubules and its identification in Mid1 and Mid2 purifications, we sought to validate these interactions. First, endogenous Astrin was immunoprecipitated (IPd) using anti-Astrin antibodies and immunoblot analysis of the IPs showed that Mid1 and Mid2 co-IPd with Astrin (Figure 1E). Next, LAP-Mid1 or Mid2 were IPd from G1/S or G2/M extracts in the presence of nocodazole (microtubule depolymerizer) and Astrin co-IPd with both Mid1 and Mid2 under both conditions, indicating that these interactions were not mediated by microtubules and were independent of the cell cycle (Figures 1F and 1G). Consistently, nocodazole treated *in vitro* binding experiments showed that HA-tagged Astrin full-length and a N-terminal fragment (amino acids (aa) 1-481) co-IPd with FLAG-tagged Mid1 and Mid2, whereas the middle region (aa 482-850) and C-terminal region (aa 851-1193) of Astrin did not interact with Mid1 or Mid2 (Figures 1H and S1). These results indicated that the N-terminus of Astrin was interacting directly with Mid1 and Mid2.

Mid1, Mid2, and Astrin Localize to Intercellular Bridge Microtubules

Astrin localizes to spindle microtubules during mitosis and intercellular bridge microtubules (ICBMTs) during cytokinesis (Mack and Compton, 2001). Thus, we asked if Mid1 or Mid2 localized to ICBMTs like Astrin. LAP-Mid1 or Mid2 expressing cells were fixed and stained for DNA, α–tubulin, and Plk1 or TPX2 or Astrin. In cytokinetic cells, LAP-Mid1 and Mid2 localized to ICBMTs partially overlapping with TPX2 and Astrin and adjacent to Plk1 staining at the midbody (Figures 2A-2F). These data indicated that the Mid1 and Mid2 localization partially overlapped with Astrin at ICBMTs during cytokinesis.

Mid1 and Mid2 are Required for Cell Division

Next we asked if Mid1 or Mid2 had a role in cell division. HeLa cells were transfected with Control (siCont) or *MID1* (siMID1) or *MID2* (siMID2) targeting siRNAs for 48 hours, fixed, and stained for DNA and α-tubulin (Figures 3A and 3B). siMID1 and siMID2 cells showed a small increase in the percentage of mitotic cells with defective spindles (multipolar and unfocused) (siMID1= 14.7±0.9, $p<.05$ and siMID2= 15±2.8, $p<.05$ compared to siCont= 9±2.2) and mitotic cells with unaligned chromosomes (where all but a

few (1-3) chromosomes were aligned at the metaphase plate) (siMID1= 9.3±2.5 , p<.05 and siMID2= 19.7±1.3, p<.0001 compared to siCont= 3.3±1.3) (Figures 3B-3D). siMID1 and siMID2 cells also showed a pronounced increase in the percentage of cells undergoing cytokinesis (siMID1= 21.7±2.9, p<.05 and siMID2= 32.7±3.4, p<.001 compared to siCont=12.0±2.0) and interphase cells with >1 nuclei (siMID1= 29.3±3.7, p<.001 and siMID2= 33±3.9, p<.001 compared to siCont= 7.3±1.9) (Figures 3B, 3E and 3F). These results indicated that depletion of Mid1 or Mid2 led to minor defects in early mitosis and major defects in cytokinesis. Consistently, live-cell time-lapse microscopy showed that siMID1 and siMID2 cells exhibited cell division defects, including cytokinetic arrest with the two cells linked by a cytokinetic bridge, a failure to divide with regression into one binucleated cell and cell division followed by death of one or both cells (Figures 3G and 3H; Movies S1-S3). siMID1 and siMID2 cells were also slower at completing abscission from the time of mitotic entry (siMID1= 4.9 ± .76 hours, p<.05 and siMID2= 6.6 ± .87 hours, p<.05 compared to siCont=3.1 ± .36 hours) (Figure 3I). Next, we asked if siMID1 and siMID2 cytokinetic defects were due to ultra-fine DNA bridges (UFBs) that go undetected by standard DNA staining (Chan et al., 2007). However, no significant increase in UFBs (visualized by staining for the BLM or PICH proteins) was seen in siMID1 or siMID2 post-metaphase cells, indicating that their cytokinetic defects were not due to UFBs (Figure S2). Together, these data indicated that depletion of Mid1 or Mid2 led to a failure to undergo proper cytokinesis, the generation of binucleated cells and cell death.

Mid2 Regulates Astrin Protein Levels

Astrin levels were reported to increase as cells entered mitosis and decrease as cells exit mitosis (Dunsch et al., 2011). Thus, it was possible that Mid1 and Mid2 were associating with Astrin to regulate Astrin levels through ubiquitination and proteasome-dependent degradation. To test this, we first verified that Astrin levels decreased during mitotic exit. G2/M arrested HeLa cells were released and protein samples were prepared at various time points and analyzed by immunoblotting. In contrast to a previous study that showed two Astrin bands (Dunsch et al., 2011), using 4-20% gradient gels, we were able to detect a third slower mobility band (Figure S3A). This third band was present in mitosis and disappeared as the cells exited mitosis concomitant with a decrease in overall Astrin levels (Figures 4A, 4B, S3B and S3C, see arrows). Next, we asked if Astrin was ubiquitinated during mitotic exit by IPing LAP-Astrin from G2/M arrested and released cells and immunoblotting for K48 and K63 ubiquitin linkages. This revealed that Astrin was modified with K48 and K63 ubiquitin linkages in early mitosis (0 hr time point) and during cytokinesis (~4 hr post release) (Figure S3D). Next, we asked if Mid1 or Mid2 had a role in regulating Astrin levels during mitotic exit. siCont, siMID1 and siMID2 treated cells were arrested in G2/M, released, and protein samples were prepared every hour for ten hours as cells exited mitosis. In siCont and siMID1 cells the modified form of Astrin and the overall Astrin levels decreased as the cells exited mitosis, whereas in siMID2 cells Astrin remained stabilized (Figures 4A and 4B, see arrows). These results indicated that Mid2 had a role in regulating Astrin levels during mitotic exit.

Next, we asked if Astrin was a Mid1 or Mid2 substrate using *in vitro* ubiquitination assays with S-35 radiolabeled Astrin and LAP-Mid1 or LAP-Mid2 expressing extracts. LAPMid2

extracts ubiquitinated Astrin, whereas LAP-Mid1 extracts were unable to (Figure 4C) and combining LAP-Mid1 and LAP-Mid2 extracts did not increase Astrin ubiquitination beyond that with LAP-Mid2 extracts (Figure S3E). Additionally, deletion of the first 80 amino acids, which contains the RING domain required for ubiquitination activity in RING domain E3 ligases, abolished Mid2's ability to ubiquitinate Astrin (Figure 4D). Interestingly, a mutant form of Mid2 where arginine 347 is mutated to glutamine (R347Q), which is found in X-linked intellectual disability patients, localized to ICBMTs, but did so rather diffusely compared to wildtype Mid2 (Figure S3F). Additionally, the R347Q mutation did not inhibit Mid2's ability to bind to (Figure S1) and ubiquitinate Astrin (Figure 4D). To map the amino acid residue/s that were ubiquitinated by Mid2, LAP-Astrin purifications from G1/S and mitotic exit (4 hr post nocodazole release) cells were analyzed by mass spectrometry. Lysine 409 (K409) of Astrin was found ubiquitinated in cells exiting from mitosis and not in G1/S cells (Figure S3G). To determine if K409 was ubiquitinated by Mid2, we first tested the ability of Mid2 to ubiquitinate full-length, N-terminal, middle, or C-terminal Astrin fragments (Figure S3H). Mid2 was only able to ubiquitinate full-length Astrin and the N-terminal fragment of Astrin that contained K409 (Figure S3H). However, Mid2 was unable to ubiquitinate Astrin (full-length or N-terminal fragment) when K409 was mutated to an alanine (K409A) (Figure S3H). These results indicated that Mid2 was ubiquitinating Astrin at K409 during mitotic exit. Consistently, whereas LAP-Astrin levels decreased during mitotic exit, LAP-Astrin-K409A remained stabilized and was degraded less efficiently (Figures 4E and 4F). Additionally, LAP-Astrin-K409A was only weakly ubiquitinated during mitotic exit (4 hrs post nocodazole release) compared to LAP-Astrin (Figure 4G). These data indicated that Mid2 was ubiquitinating Astrin at K409 and targeting Astrin for degradation during cytokinesis.

The Mid2 Ubiquitination Resistant Astrin-K409A Mutant Inhibits Cytokinesis

To further establish that Mid2 regulated cell division through ubiquitination of Astrin on K409, we analyzed the consequences of expressing Astrin-K409A on cell division. Overexpression of either LAP-Astrin or LAP-Astrin-K409A led to cell division defects (Figure S4A and S4B). Interestingly, cells depleted of endogenous Astrin (using anti-ASTRIN siRNAs, Figure S4C) that expressed siRNA resistant LAP-Astrin underwent proper cytokinesis, while those expressing siRNA resistant LAP-Astrin-K409A arrested during cytokinesis (LAP-Astrin= 22±4.5% compared to LAP-Astrin-K409A=42±4.9%, $p<.05$) (Figures 4H and 4I). LAP-Astrin-K409A also spread to a larger area on ICBMTs during cytokinesis (Figure 4H) and fluorescence intensity measurements showed that LAP-Astrin-K409A accumulated at ICBMTs compared to LAP-Astrin (LAP-Astrin= 135.6±46.1 (A.U.) compared to LAP-Astrin-K409A=386±96.7 (A.U.), $p<.05$) (Figure 4J). LAP-Astrin-K409A expressing cells also had an increased percentage of interphase cells with >1 nuclei (mostly binucleate) compared to LAP-Astrin expressing cells (LAP-Astrin= 15±2.5 compared to LAP-Astrin-K409A=30±4.3, $p<.05$) (Figure 4K) and an increased percentage of dead cells (LAP-Astrin= 12±2.9 compared to LAP-Astrin-K409A=23±2.5, $p<.05$) (Figure 4L). These data indicated that in Astrin depleted cells expression of LAP-Astrin promoted cytokinesis, whereas LAP-Astrin-K409A was stabilized during cytokinesis at ICBMTs leading to cytokinetic arrest, cytokinetic failure, the generation of binucleated cells and an increase in cell death. Interestingly, similar LAP-Astrin and LAP-Astrin-K409A levels were observed

during early mitosis in siCont, siMID1 and siMID2 treated cells by immunofluorescence, indicating that Mid1 or Mid2 were not regulating the levels of Astrin in early mitosis (Figures S4D and S4E). However, LAP-Astrin and LAP-Astrin-K409A levels were elevated in siMID2 cells at ICBMTs (Figure S4F). Finally, we analyzed the interdependencies of Mid1, Mid2, and Astrin for their localization to ICBMTs. Each protein was able to localize to ICBMTs independent of the others, indicating that they did not rely on each other for their localization to ICBMTs (Figures S4E and S4G).

DISCUSSION

This study aimed to increase our understanding of the molecular basis of X-linked developmental disorders associated with mutation of the *MID1* and *MID2* ubiquitin ligases. We determined that Mid1 and Mid2 bound directly to the N-terminus of Astrin and their localization overlapped with Astrin at ICBMTs during cytokinesis. Further, Astrin was ubiquitinated during cytokinesis at K409 in a Mid2-dependent manner and this modification was necessary to degrade a pool of Astrin. Consistently, Mid2 depletion led to the stabilization of Astrin during cell division, cytokinetic arrest, the generation of binucleate cells that failed cytokinesis and cell death. Furthermore, expression of mutant Astrin-K409A, led to its stabilization during cell division, its accumulation at ICBMTs, cytokinetic defects and cell death. These data indicate that Mid2 promotes cell division through ubiquitination of Astrin on K409. Finally, these data indicate that Mid2 may regulate microtubule organization through the ubiquitination and destruction of Astrin, which helps to explain how mutation of *MID2* can lead to the misregulation of microtubule organization and the downstream disease pathology that is associated with patients with X-linked intellectual disabilities (XLID). Interestingly, the Mid2 missense mutation R347Q that has been linked to XLID (abolishes Mid2 microtubule binding (Geetha et al., 2014)), localized to ICBMTs, but did so rather diffusely compared to wildtype Mid2, was able to bind to and ubiquitinate Astrin *in vitro*. Therefore, the R347Q mutation does not appear to interfere with Mid2 ubiquitination activity or Mid2 substrate binding and instead interferes with the ability of Mid2 to localize to its proper subcellular location where its activity is required.

Several questions remain regarding Mid1 and Mid2 and their regulation of microtubules and cell division. First, Mid1 does not appear to be regulating Astrin levels and we were unable to identify Mid1 specific interactors that would explain its role in cytokinesis, thus it will be important to determine if Mid1 has a direct influence on a process that regulates cell division or if it has substrates that regulate cell division that are as yet unidentified. Second, the Mid2 interactome also identified ASPM (Abnormal Spindle-like, Microcephaly-associated) and CEP128 (Centromeric Protein 128), which associate with centrosomes and ASPM has also been linked to the regulation of spindle assembly and cytokinesis (Higgins et al., 2010; Jakobsen et al., 2011; Paramasivam et al., 2007), thus these proteins should be explored further as potential Mid2 substrates.

EXPERIMENTAL PROCEDURES

Cell Culture and Cell Cycle Synchronization

Cell line growth and siRNA treatments with Dharmacon control non-targeting siRNA (D-001810-10) and siRNAs targeting *MID1* (D-006537-1), *MID2* (D-006938-03) and *ASTRIN* (J-006839-05-08) were used as described previously (Torres et al., 2010). For G1/S arrest and release experiments, cells were arrested with 2mM thymidine for 18 hours, washed 3 times with PBS and 2 times with complete media and released into fresh media. For G2/M arrest and release experiments, cells were arrested with 330nM nocodazole for 16 hours, washed 3 times with PBS and 2 times with complete media and released into fresh media.

Plasmids, Mutagenesis, and Generation of Stable Cell Lines

For full-length MID1/MID2/MID2-Δ80/MID2-R347Q/ASTRIN/ASTRIN-K409A/ LUCIFERASE or *ASTRIN/ASTRIN-K409A* truncation expression, their cDNA was fused to the c-terminus of either HA (pCS2-HA-DEST), EGFP (pGLAP1) or FLAG (pCS2-FLAG-DEST) as described previously (Torres et al., 2011). pGLAP1-*MID1/MID2/ASTRIN/ ASTRIN-K409A* were used to generate doxycycline inducible HEK293 or HeLa Flp-In T-REx LAP-*MID1/MID2/ASTRIN/ASTRIN-K409A* stable cell lines that express the fusion protein from a single genetic locus as described previously (Torres et al., 2009).

LAP Purifications, Identification of Mid1 and Mid2 Associated Proteins by LC-MS/MS, and Immunoprecipitations

LAP purifications, the identification of Mid1 and Mid2 associated proteins and the identification of ubiquitination sites on Astrin by LC-MS/MS, and immunoprecipitations were as described previously (Torres et al., 2009). Briefly, LAP-Mid1 or LAP-Mid2 cell lines were induced with .1μg/ml Dox for 16 hours and cells were harvested and lysed. Cleared lysates were subjected to tandem affinity purifications by incubation with anti-GFP antibody beads and bound eluates were incubated with S protein agarose. Final eluates were resolved on a 4-20% SDS-PAG and 10 gel slices corresponding to the entire lane of the SDS PAG were excised and prepared for examination by mass spectrometry. For mapping the Astrin mitotic ubiquitination site LAP-Astrin was purified from thymidine arrested or cells released from nocodazole for 4 hours and tandem affinity purified as described above. Mass spectrometry analyses were performed at the Harvard Mass Spectrometry and Proteomics Resource Laboratory by microcapillary reverse-phase HPLC nano-electrospray tandem mass spectrometry (μLC/MS/MS) on a Thermo LTQ-Orbitrap mass spectrometer as described in (Vanderwerf et al., 2009), or at the UCLA Pasarow Mass Spectrometry Laboratory on a Thermo LTQ-Orbitrap XL as described in (Patananan et al., 2014). For details, see Supplemental Experimental Procedures.

Ubiquitination Reactions

Ubiquitination reactions were as described previously (Senese et al., 2015), except that recombinant Astrin was incubated with mitotic HEK293, LAP-Mid1 or LAP-Mid2 cell extracts. For details, see Supplemental Experimental Procedures.

Immunofluorescence and Live-cell Time-lapse Microscopy

Immunofluorescence microscopy was carried out as described previously (Torres et al., 2010). HeLa or HEK293 stable cell lines were induced to express Mid1 or Mid2 for 24 hours and fixed, permeabilized, and co-stained with the indicated antibodies. Images were captured with a Leica DMI6000 microscope (Leica DFC360 FX Camera, 63×/1.40-0.60 NA oil objective, Leica AF6000 software). Images were deconvolved with Leica Application Suite 3D Deconvolution software and exported as TIFF files. For quantifying spindle and cytokinetic defects, 100 cells from 3 independent experiments were counted and the data are presented as the average ± SD. For time-lapse microscopy, HeLa cells were transfected with indicated siRNAs for 24 hours, arrested in G1/S with 2 mM thymidine for 18 hours, washed, and released. Cells were imaged live 5 hours post release for 20 hours using a Leica DMI6000 microscope, described above, at 37 °C, and 5% CO_2 using a 20×/0.4 NA air objective. Images were converted to AVI movies. Each frame represents a five-minute interval. For details and a list of antibodies used, see Supplemental Experimental Procedures.

Supplementary Material

Refer to Web version on PubMed Central for supplementary material.

ACKNOWLEDGEMENTS

This work was supported by a National Science Foundation Grant MCB1243645 to J.Z.T., and by a UCSD/UCLA DRC P30 DK063491 grant to J.P.W.

REFERENCES

Berti C, Fontanella B, Ferrentino R, Meroni G. Mig12, a novel Opitz syndrome gene product partner, is expressed in the embryonic ventral midline and co-operates with Mid1 to bundle and stabilize microtubules. BMC Cell Biol. 2004; 5:9. [PubMed: 15070402]

Cainarca S, Messali S, Ballabio A, Meroni G. Functional characterization of the Opitz syndrome gene product (midin): evidence for homodimerization and association with microtubules throughout the cell cycle. Hum Mol Genet. 1999; 8:1387–1396. [PubMed: 10400985]

Chan KL, North PS, Hickson ID. BLM is required for faithful chromosome segregation and its localization defines a class of ultrafine anaphase bridges. EMBO J. 2007; 26:3397–3409. [PubMed: 17599064]

Du H, Huang Y, Zaghlula M, Walters E, Cox TC, Massiah MA. The MID1 E3 ligase catalyzes the polyubiquitination of Alpha4 (alpha4), a regulatory subunit of protein phosphatase 2A (PP2A): novel insights into MID1-mediated regulation of PP2A. J Biol Chem. 2013; 288:21341–21350. [PubMed: 23740247]

Dunsch AK, Linnane E, Barr FA, Gruneberg U. The astrin-kinastrin/SKAP complex localizes to microtubule plus ends and facilitates chromosome alignment. J Cell Biol. 2011; 192:959–968. [PubMed: 21402792]

Geetha TS, Michealraj KA, Kabra M, Kaur G, Juyal RC, Thelma BK. Targeted deep resequencing identifies MID2 mutation for X-linked intellectual disability with varied disease severity in a large kindred from India. Hum Mutat. 2014; 35:41–44. [PubMed: 24115387]

Gruber J, Harborth J, Schnabel J, Weber K, Hatzfeld M. The mitotic-spindle-associated protein astrin is essential for progression through mitosis. J Cell Sci. 2002; 115:4053–4059. [PubMed: 12356910]

Higgins J, Midgley C, Bergh AM, Bell SM, Askham JM, Roberts E, Binns RK, Sharif SM, Bennett C, Glover DM, et al. Human ASPM participates in spindle organisation, spindle orientation and cytokinesis. BMC Cell Biol. 2010; 11:85. [PubMed: 21044324]

Jakobsen L, Vanselow K, Skogs M, Toyoda Y, Lundberg E, Poser I, Falkenby LG, Bennetzen M, Westendorf J, Nigg EA, et al. Novel asymmetrically localizing components of human centrosomes identified by complementary proteomics methods. EMBO J. 2011; 30:1520–1535. [PubMed: 21399614]

Mack GJ, Compton DA. Analysis of mitotic microtubule-associated proteins using mass spectrometry identifies astrin, a spindle-associated protein. Proc Natl Acad Sci U S A. 2001; 98:14434–14439. [PubMed: 11724960]

Meroni G, Diez-Roux G. TRIM/RBCC, a novel class of 'single protein RING finger' E3 ubiquitin ligases. Bioessays. 2005; 27:1147–1157. [PubMed: 16237670]

Paramasivam M, Chang YJ, LoTurco JJ. ASPM and citron kinase co-localize to the midbody ring during cytokinesis. Cell Cycle. 2007; 6:1605–1612. [PubMed: 17534152]

Patananan AN, Capri J, Whitelegge JP, Clarke SG. Non-repair Pathways for Minimizing Protein Isoaspartyl Damage in the Yeast Saccharomyces cerevisiae. J Biol Chem. 2014; 289:16936–16953. [PubMed: 24764295]

Schweiger S, Dorn S, Fuchs M, Kohler A, Matthes F, Muller EC, Wanker E, Schneider R, Krauss S. The E3 ubiquitin ligase MID1 catalyzes ubiquitination and cleavage of Fu. J Biol Chem. 2014; 289:31805–31817. [PubMed: 25278022]

Senese S, Cheung K, Lo YC, Gholkar AA, Xia X, Wohlschlegel JA, Torres JZ. A unique insertion in STARD9's motor domain regulates its stability. Mol Biol Cell. 2015; 26:440–452. [PubMed: 25501367]

Short KM, Cox TC. Subclassification of the RBCC/TRIM superfamily reveals a novel motif necessary for microtubule binding. J Biol Chem. 2006; 281:8970–8980. [PubMed: 16434393]

Short KM, Hopwood B, Yi Z, Cox TC. MID1 and MID2 homo- and heterodimerise to tether the rapamycin-sensitive PP2A regulatory subunit, alpha 4, to microtubules: implications for the clinical variability of X-linked Opitz GBBB syndrome and other developmental disorders. BMC Cell Biol. 2002; 3:1. [PubMed: 11806752]

Suzuki M, Hara Y, Takagi C, Yamamoto TS, Ueno N. MID1 and MID2 are required for Xenopus neural tube closure through the regulation of microtubule organization. Development. 2010; 137:2329–2339. [PubMed: 20534674]

Thein KH, Kleylein-Sohn J, Nigg EA, Gruneberg U. Astrin is required for the maintenance of sister chromatid cohesion and centrosome integrity. J Cell Biol. 2007; 178:345–354. [PubMed: 17664331]

Torres JZ, Ban KH, Jackson PK. A Specific Form of Phospho Protein Phosphatase 2 Regulates Anaphase-promoting Complex/Cyclosome Association with Spindle Poles. Mol Biol Cell. 2010; 21:897–904. [PubMed: 20089842]

Torres JZ, Miller JJ, Jackson PK. High-throughput generation of tagged stable cell lines for proteomic analysis. Proteomics. 2009; 9:2888–2891. [PubMed: 19405035]

Torres JZ, Summers MK, Peterson D, Brauer MJ, Lee J, Senese S, Gholkar AA, Lo YC, Lei X, Jung K, et al. The STARD9/Kif16a Kinesin Associates with Mitotic Microtubules and Regulates Spindle Pole Assembly. Cell. 2011; 147:1309–1323. [PubMed: 22153075]

Trockenbacher A, Suckow V, Foerster J, Winter J, Krauss S, Ropers HH, Schneider R, Schweiger S. MID1, mutated in Opitz syndrome, encodes an ubiquitin ligase that targets phosphatase 2A for degradation. Nat Genet. 2001; 29:287–294. [PubMed: 11685209]

Vanderwerf SM, Svahn J, Olson S, Rathbun RK, Harrington C, Yates J, Keeble W, Anderson DC, Anur P, Pereira NF, et al. TLR8-dependent TNF-(alpha) overexpression in Fanconi anemia group C cells. Blood. 2009; 114:5290–5298. [PubMed: 19850743]

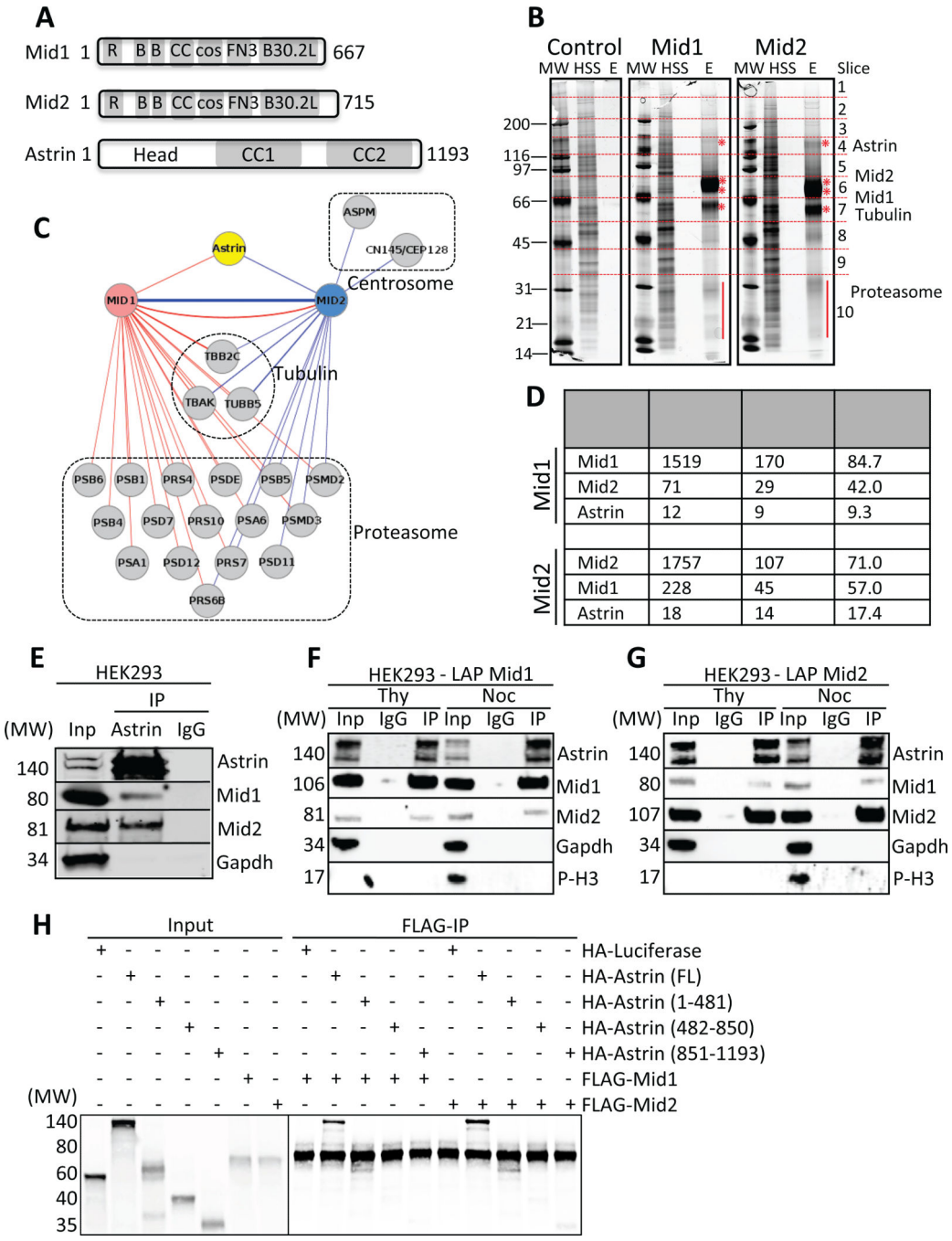

Figure 1. Astrin Associates with Mid1 and Mid2

(A) Mid1, Mid2 and Astrin domain architecture with the number of amino acids indicated. R= RING finger, B= B-box, CC= coiled coil, cos= C-terminal subgroup one signature box, FN3= fibronectin type III, B30.2L= B30.2-like/RFP (Ret finger protein motif), and CC1/2= coiled coil 1/2.

(B) Silver stained gels of control (LAP only), LAP-Mid1 and LAP-Mid2 tandem affinity purifications. MW= molecular weight, HSS= high spin supernatant, E= eluates. Protein

bands corresponding to Mid1, Mid2, Astrin, tubulin and proteasome subunits are indicated. The ten gel slices analyzed by LC-MS/MS are indicated with red lines.

(C) Mid1 (red) and Mid2 (blue) interactomes visualized with Cytoscape showing the four major categories of interacting proteins; tubulin isoforms, proteasome subunits, centrosome proteins and Astrin. For details see Table S1.

(D) Summary of mass spectrometry data showing the top Mid1 and Mid2 interactors including protein name, number of peptides identified, number of unique peptides and the percent protein coverage.

(E) IPs from HEK293 cell extracts using anti-Astrin or control IgG antibodies were immunoblotted with the indicated antibodies. Note that Mid1 and Mid2 co-IP with endogenous Astrin.

(F-G) Anti-GFP antibodies were used to perform IPs from LAP-Mid1 (F) or LAP-Mid2 (G) cell extracts prepared from thymidine or nocodazole arrested cells in the presence of nocodazole. IPs were immunoblotted with the indicated antibodies. Note that Mid2 and Astrin co-IP with LAP-Mid1 (F) and Mid1 and Astrin co-IP with LAP-Mid2 (G).

(H) *In vitro* IPs with S-35 radiolabeled HA-tagged Astrin (full-length and indicated fragments) or Luciferase and FLAG-tagged Mid1 or Mid2. Note that Astrin (full-length and 1-481) co-IPs with both Mid1 and Mid2. See also Figure S1.

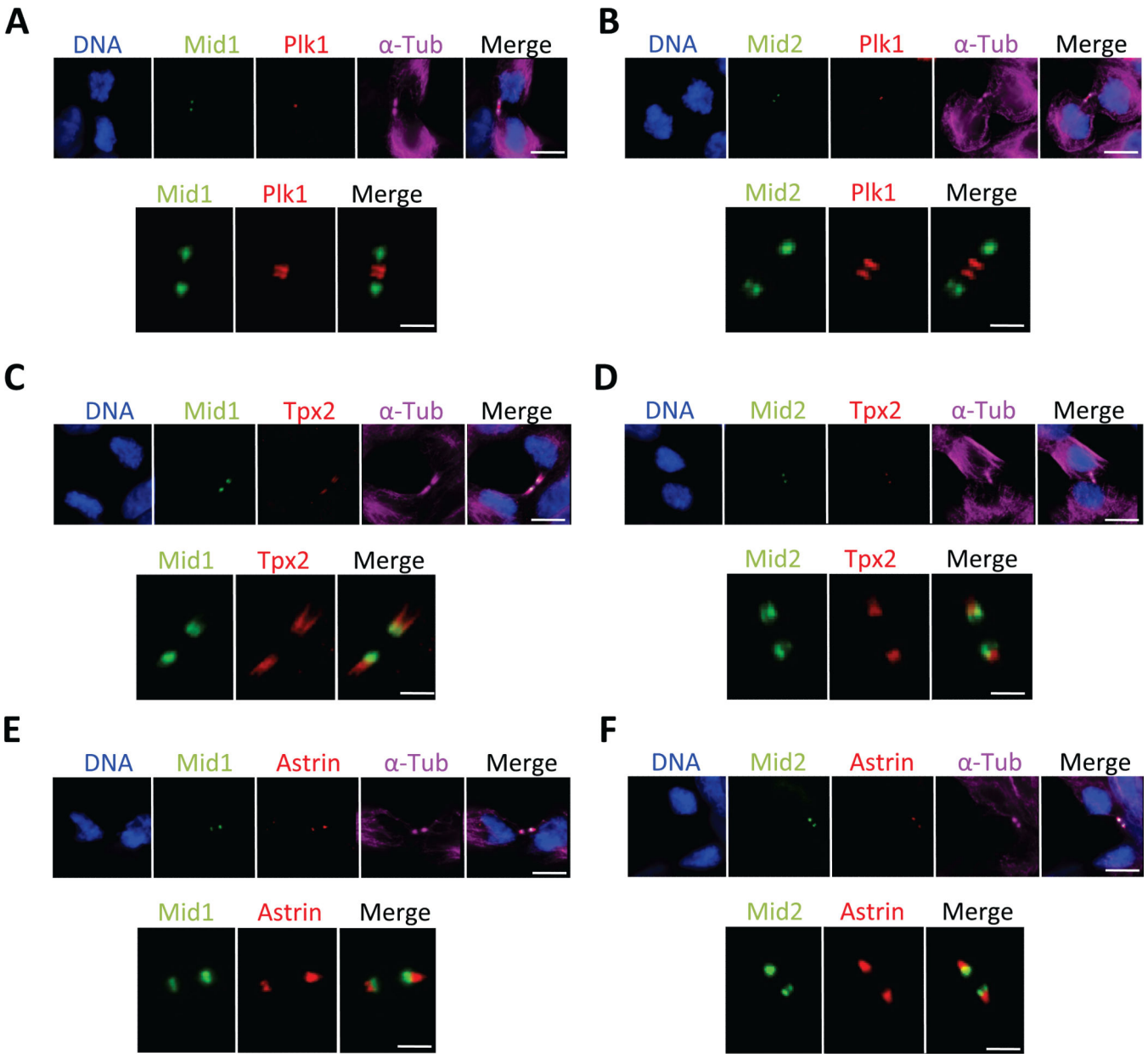

Figure 2. The Localization of Mid1, Mid2 and Astrin Overlaps at ICBMTs

(A-F) Immunofluorescence microscopy of LAP-Mid1 or Mid2 expressing cells stained for DNA, α–tubulin, and Plk1 (A-B) or TPX2 (C-D) or Astrin (E-F). Note that Mid1 and Mid2 localize to ICBMTs overlapping with TPX2 and Astrin and adjacent to the Plk1 midbody staining. Scale bar= 5μm. Lower panels show zoom images of the cytokinetic bridge region. Scale bar= 2μm.

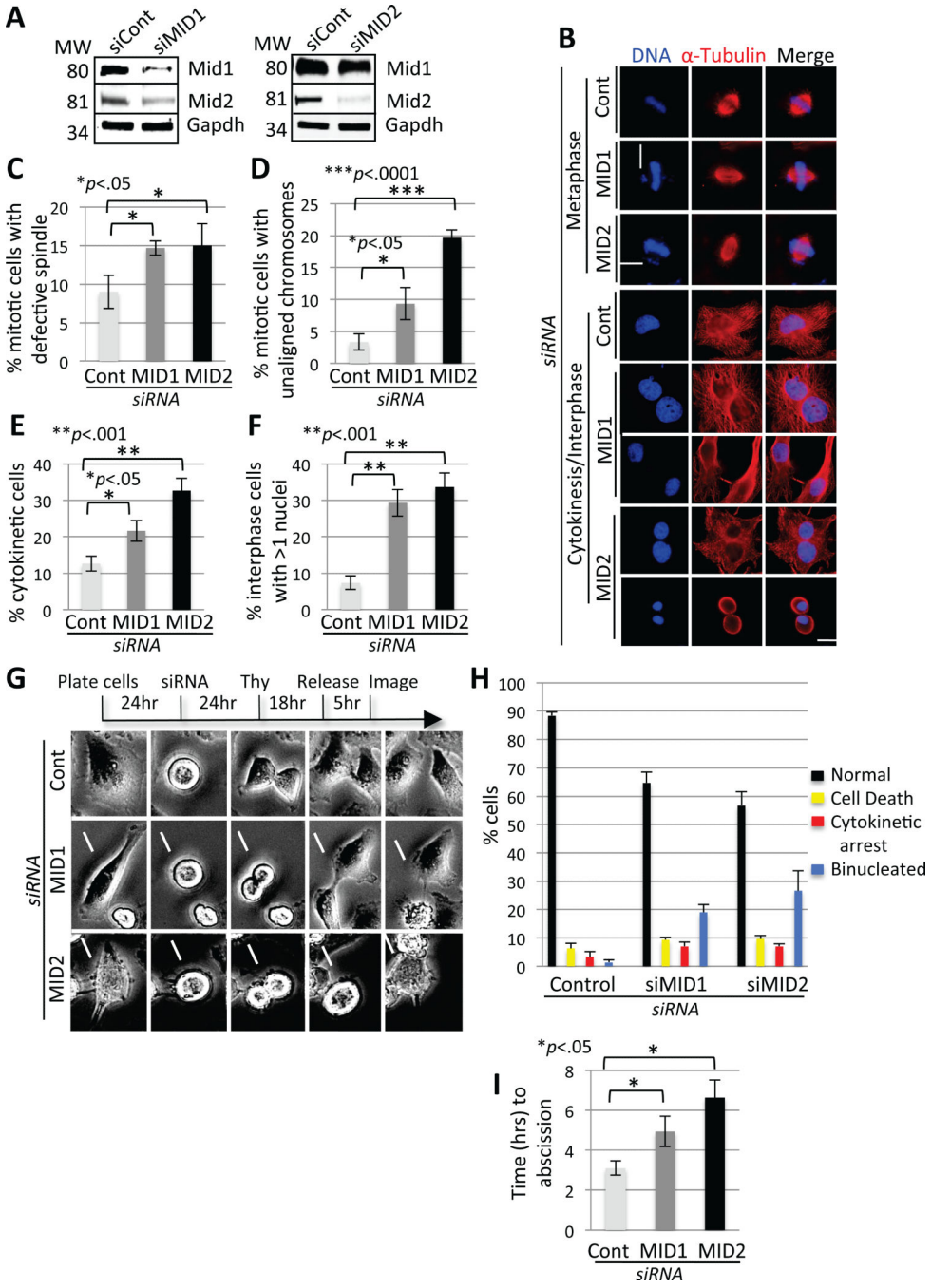

Figure 3. Depletion of Mid1 or Mid2 Leads to Cytokinetic Defects

(A) Immunoblot analysis showing that siRNA oligonucleotides targeting MID1 (siMID1) or MID2 (siMID2) deplete Mid1 or Mid2 compared to control non-targeting siRNAs (siCont). (B) Immunofluorescence microscopy of HeLa cells treated with siCont, siMID1, or siMID2 for 48 hrs and stained for DNA and α-tubulin. Note that siMID1 and siMID2 cells have unaligned chromosomes, arrest during cytokinesis and have an increased number of binucleated cells. Scale bar = 5μm.

(C) Quantification of the percentage of cells with defective spindles. Data represent average ± SD of 3 independent experiments, 100 cells counted for each. (*) $p< 0.05$.
(D) Same as in (C), except that the percentage of mitotic cells with unaligned chromosomes was quantified. (*) $p< 0.05$ and (***) $p< 0.001$.
(E) Same as in (C), except that the percentage of cytokinetic cells was quantified. (*) $p< 0.05$ and (**) $p< 0.001$.
(F) Same as in (C), except that the percentage of cells with >1 nuclei was quantified. (**) $p< 0.001$.
(G) Live-cell time-lapse microscopy snapshots of HeLa cells treated with siCont, siMID1 or siMID2. Representative cell division defects are shown, including cytokinetic arrest, cell death and regression of dividing cells into binucleated cells. Time is in minutes. See also Movies S1-S3.
(H) The percentage of cells undergoing normal cell division, arresting during cytokinesis, dying during cell division and failing cytokinesis and regressing to a binucleated state were quantified for siCont, siMID1 or siMID2 treated cells. Data represent the average ± SD of 3 independent experiments, 50 cells counted for each.
(I) Quantification of the time between mitotic entry and cell abscission for siCont, siMID1 or siMID2 treated cells. Data represent the average ± SD of 3 independent experiments, 50 cells counted for each. (*) $p< 0.05$. See also Figure S2.

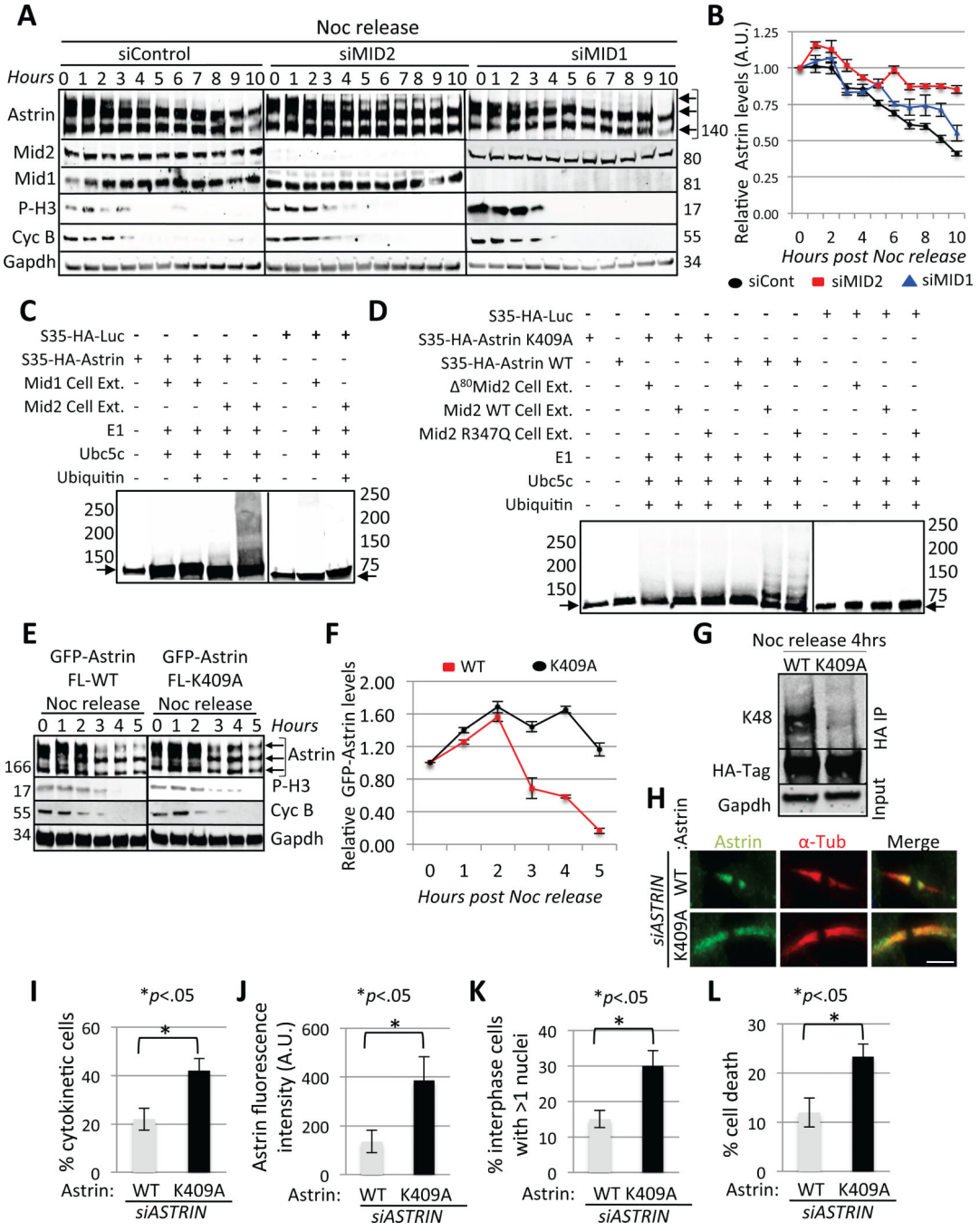

Figure 4. Mid2 Regulates Astrin Levels in a Cell Cycle Dependent Manner

(A-B) Analysis of Astrin levels during mitotic exit. HeLa cells treated with control siRNA (siControl) or siRNA targeting Mid1 (siMID1) or Mid2 (siMID2) were arrested in G2/M with nocodazole, released and harvested at the indicated time points. Protein extracts were then analyzed by immunoblotting with the indicated antibodies. Note that in siCont cells, Mid1 and Mid2 protein levels remain constant, whereas Astrin levels decrease as cells exit mitosis. Also note that siMID2 cells stabilize Astrin during mitotic exit. Immunoblots shown are representative data from one of three independent experiments. (B) Quantification of

Astrin levels during mitotic exit from (A). Data represent the average ± SD of 3 independent experiments. See also Figure S3.

(C) *In vitro* ubiquitination assays were performed with or without S-35 radiolabeled recombinant HA-Astrin or HA-Luciferase (HA-Luc, negative control) and LAP-Mid1 or LAP-Mid2 expressing extracts. Reactions were resolved by SDS-PAGE, transferred onto a PVDF membrane and ubiquitination was monitored by radiometric analyses. Note that a smear of higher molecular weight bands appears in the reaction with LAP-Mid2 expressing extracts, indicative of Astrin ubiquitination. See also Figure S3.

(D) *In vitro* ubiquitination assays performed as in (C) with LAP-Mid2-WT or Δ80 (first 80 amino acids deleted) or R347Q (point mutation) expressing extracts.

(E-F) HeLa cells expressing LAP-Astrin-WT or LAP-Astrin-K409A were arrested in G2/M with nocodazole, released and harvested at the indicated time points. Protein extracts were then analyzed by immunoblotting with the indicated antibodies. Note that LAP-Astrin-WT is degraded during mitotic exit, whereas LAP-Astrin-K409A remains stabilized. Immunoblots shown are representative data from one of three independent experiments. (F) Quantification of LAP-Astrin-WT and LAP-Astrin-K409A levels during mitotic exit from (E). Data represent the average ± SD of 3 independent experiments.

(G) HeLa cells expressing HA-Astrin-WT or HA-Astrin-K409A were released form nocodazole arrest and HA-Astrin was IPd with anti-HA antibodies during mitotic exit (4 hours post release). Immunoprecipitates were immunoblotted with anti-K48 ubiquitin chain antibodies. Note that wildtype HA-Astrin was ubiquitinated robustly, whereas mutant HA-Astrin-K409A was only minimally ubiquitinated. See also Figure S3.

(H) Endogenous Astrin proteins levels were depleted with siRNA targeting Astrin (siASTRIN) and LAP-Astrin-WT or LAP-Astrin-K409A were expressed. Cells were then fixed and stained for microtubules (anti-α-tubulin antibodies) and LAP-Astrin (anti-GFP antibodies). Scale bar= 2μm. See also Figure S4.

(I) Quantification of the percentage of cells arrested at cytokinesis. Data represent the average ± SD of 3 independent experiments, 100 cells counted for each. (*) $p < 0.05$.

(J) Quantification of the total fluorescence intensity of LAP-Astrin or LAP-Astrin-K409A at the cytokinetic bridge. Data represent the average ± SD of 3 independent experiments, 50 cells counted for each. (**) $p < 0.005$, A.U.= arbitrary units. See also Figure S4.

(K) Quantification of the percentage of interphase cells with >1 nuclei was quantified. Data represent the average ± SD of 3 independent experiments, 100 cells counted for each. (*) $p < 0.05$.

(L) Quantification of the percent cell death. Data represent the average ± SD of 3 independent experiments, 100 cells counted for each. (*) $p < 0.05$.